1993ApJ...406L..29W

THE ASTROPHYSICAL JOURNAL, 406:L29–L33, 1993 March 20
© 1993. The American Astronomical Society. All rights reserved. Printed in U.S.A.

N_2H^+ IN THE ORION AMBIENT RIDGE: CLOUD CLUMPING VERSUS ROTATION

MARIA WOMACK,[1] L. M. ZIURYS,[2,3] AND L. J. SAGE[4,5]
Received 1992 September 21; accepted 1993 January 7

ABSTRACT

Spectra of the $J = 1 \rightarrow 0$ transition of N_2H^+ have been obtained over a $2' \times 2'$ area toward the Orion-KL/IRc2 star-forming region with 26″ angular resolution using the IRAM 30 m telescope. The N_2H^+ emission, which exclusively traces the ridge gas, exhibits multiple radial velocities which appear to arise from the presence of at least four clouds of quiescent material. One cloud, ~75″ in extent, lies to the N and NE of Orion-KL, with a velocity of $V_{LSR} \sim 9.5$ km s^{-1}. A second cloud, ~60″ in extent, lies to the NW and W, with an average velocity of $V_{LSR} \sim 7.2$ km s^{-1}. There appears to be such a sharp velocity discontinuity between these two clouds that both velocity components are present within a 15″ region centered near IRc2 and other infrared sources. A third region, ~35″ in extent, with $V_{LSR} \sim 8.1$ km s^{-1}, is seen ~15″ S of IRc2 and is likely to arise from the compact ridge. A fourth velocity component of $V_{LSR} \sim 6.4$ km s^{-1} lies 15″–30″ SW of IRc2 and is attributed to Orion-S. The velocity structure of N_2H^+, therefore, does not uniformly change across OMC-1 and, consequently, is inconsistent with the presence of large-scale (~1′–2′) differential rotation of the extended ridge along the SW–NE axis about IRc2. The coincidence of the two larger clouds with star-forming activity in Orion-KL suggests that either the quiescent gas is being pushed apart or that the star formation may have been triggered by a cloud-cloud interaction.

Subject headings: ISM: clouds — ISM: individual: Orion-KL — ISM: molecules — ISM: structure — stars: formation

1. INTRODUCTION

Star formation is a fundamental problem in astronomy which remains poorly understood. One of the best studied sites of active star formation is the nearby Orion Molecular Cloud (OMC-1), which contains Orion-KL, a region with several strong compact infrared sources, at least one young stellar object, IRc2, molecular outflows, and masers (e.g., Downes et al. 1981; Snell et al. 1984; Johnston et al. 1992). The extended, quiescent gas of OMC-1 is usually referred to as the ridge or spike component.

The structure of the quiescent gas is not well understood. A shift in radial velocity from ~7 to 10 km s^{-1} along the SW–NE direction of the extended ridge has been observed. While observations of some molecules, such as CO, CS and HCN, suggest that this velocity shift arises from overall rotation of the quiescent gas (e.g., Liszt et al. 1974; Hasegawa et al. 1984; Vogel et al. 1985), data on NH_3, H_2CO, and SO are better explained by the presence of two separate clouds (Ho & Barrett 1978; Bastien et al. 1981, 1985; Friberg 1984). Unfortunately, most of the molecules studied toward Orion-KL thus far are present in the hot, energetic outflows as well as in the extended ridge gas, which makes it almost impossible to trace the ambient gas near the star-forming activity. In order to better understand the large-scale dynamics of the ridge near IRc2, it is important to observe molecules which can be found *only* in the quiescent gas.

One molecule with great potential for yielding information about the extended ridge is N_2H^+, which is an excellent tracer of cold, dense, quiescent regions (Womack, Ziurys, & Wyckoff 1992). Low angular resolution (70″) observations of N_2H^+ toward Orion-KL indicate that the ridge gas consists of at least two separate clouds with a possible juncture near IRc2 (Womack, Ziurys, & Wyckoff 1991). These data, although taken with low spatial resolution, imply that there is no large-scale differential rotation of the ridge gas.

In order to probe the quiescent gas near IRc2 in closer detail, and to examine the question of the rotation, we have observed the $J = 1 \rightarrow 0$ transition of N_2H^+ toward Orion-KL with 26″ resolution using the IRAM 30 m telescope. Here we present the spectra and discuss implications for large-scale dynamics and star formation in OMC-1.

2. OBSERVATIONS

Spectra of the N_2H^+ $J = 1 \rightarrow 0$ transition were obtained using the Institut de Radio Astronomie Millimétrique (IRAM) 30 m telescope at Pico Veleta in Spain during UT 1990 August 10–12, 1991 August 14–15, and 1991 November 2–3. The $\lambda = 3$ mm SIS receiver was used, with a system temperature of $T_{sys} \sim 550$ K at 93.1710 GHz. The spectrometer consisted of a 256 channel filterbank with 100 kHz resolution, corresponding to a velocity resolution of 0.32 km s^{-1} per channel. The half-power beam width at this frequency was $\theta_b = 26''$, and the beam efficiency was $\eta_b \sim 0.6$. Temperature scales were established by the chopper-wheel method and are given in terms of T_A^*. The spectra were obtained in a dual position-switching mode, with the off position ±900″ in azimuth. Maps of N_2H^+ emission were made in a $2' \times 2'$ grid across OMC-1, centered on $\alpha = 5^h32^m46^s.7$; $\delta = 5°24'23''.0$ (1950.0). The pointing accuracy is estimated to be ~5″. All scans at each offset position were averaged, and a baseline of order zero or one was subtracted from them.

[1] Department of Physics and Astronomy, Northern Arizona University, Flagstaff, AZ 86011-6010.
[2] Department of Chemistry, Arizona State University, Tempe, AZ 85287-1604.
[3] Presidential Faculty Fellow.
[4] Max-Planck-Institut für Radioastronomie, Auf Dem Hugel 69, W-5300 Bonn 1, Germany.
[5] Now at Department of Physics, University of Nevada, Las Vegas, Las Vegas, NV 89154.

© American Astronomical Society • Provided by the NASA Astrophysics Data System

1993ApJ...406L..29W

3. RESULTS

The N_2H^+ $J = 1 \rightarrow 0$ transition consists of seven hyperfine lines which are collapsed into three ΔF_1 components (Cazzoli et al. 1985). Figure 1 shows N_2H^+ spectra toward OMC-1 as a function of position on the sky. The three ΔF_1 hyperfine components can be seen clearly at the position $(\Delta\alpha'', \Delta\delta'') = (-30, 30)$.

In order to measure the N_2H^+ radial velocities, the three ΔF_1 line regions were defined and Gaussian profiles were fitted to the data. If two different velocity components were present in a single spectrum [i.e., at $(-15, 15)$], then Gaussian profiles were fitted to all six features to deconvolve the lines. The resulting velocities are indicated for each position in Figure 1 and are listed in Table 1. The $\Delta F_1 = -1$ line is the only transition which has no further hyperfine splitting and, consequently, was used for determining the N_2H^+ line width. For the few spectra in which the $\Delta F_1 = -1$ line could not be clearly seen, line widths were measured for the $\Delta F_1 = 0$ and $+1$ transitions, and the width of the $\Delta F_1 = -1$ line was estimated. Line radiation temperatures and line widths are listed in Table 1. Uncertainties in velocity and line-width measurements were determined from the Gaussian fits, and the accuracy of the radiation temperatures is estimated to be $\pm 15\%$.

As demonstrated by Figure 1 and Table 1, there appear to be four distinct velocity components of the quiescent gas within $\sim 30''$ of IRc2. To the N and NE is a 9.5 ± 0.3 km s^{-1} component which traces a cloud $\sim 75''$ in extent. To the N, W, and NW of the infrared source is a 7.2 ± 0.3 km s^{-1} cloud with a size of $\sim 60''$. The linear scale of these clouds is ~ 0.15 pc, assuming a distance of 480 pc to Orion-KL. There is a noticeable overlap of the 9.5 and 7.2 km s^{-1} velocities within our $26''$ beam at the positions (0, 0), (0, 15), $(-15, 15)$, and $(-15, 0)$. A third, more confined component, with $V_{LSR} = 8.1 \pm 0.3$ km s^{-1}, is seen $\sim 15''$ S of IRc2 and extends about $35''$. A fourth component, at $V_{LSR} = 6.4 \pm 0.2$ km s^{-1}, is observed more than $20''$ to the S and SW of Orion-KL. The line widths of the 9.5 and 7.2 km s^{-1} components are $\Delta v_{1/2} = 1.1 \pm 0.1$ km s^{-1}, while the 8.1 and 6.4 km s^{-1} components are slightly broader at 1.2 ± 0.2 and 1.3 ± 0.3 km s^{-1}, respectively. Another interesting feature of the map is the significant decrease in N_2H^+ near the (0, 0) position, compared with only $30''$ N or W, and the absence of emission to the E and SE of IRc2.

4. DISCUSSION

4.1. *Multiple Cloud Components versus Ridge Rotation*

Four separate velocity components in N_2H^+ of ~ 9.5, 8.1, 7.2, and 6.4 km s^{-1} are present in OMC-1 and must all arise from the ridge because of their narrow line widths. The 8.1 km s^{-1} cloud clump has a radial velocity, angular size, and location similar to the so-called compact ridge, although it has a somewhat narrow line width for this region (e.g., Blake et al. 1987; Mangum et al. 1990). The 6.4 km s^{-1} component is attributed to Orion-S which has a radial velocity of ~ 6.5 km

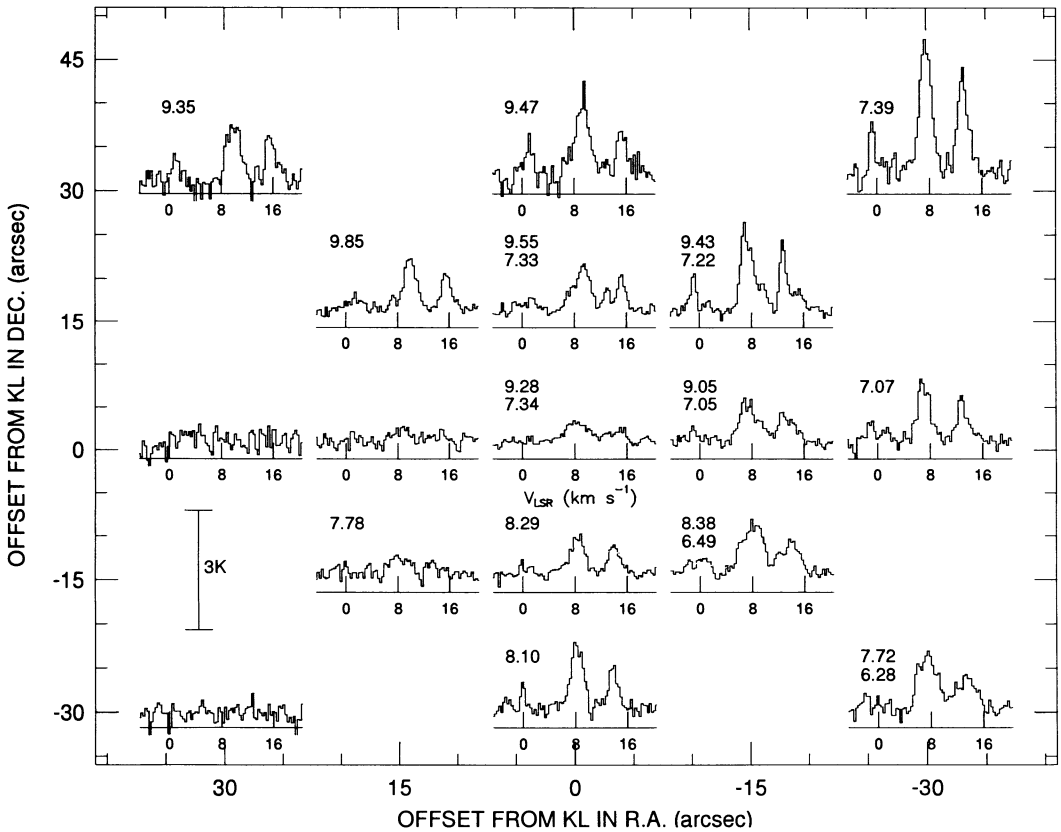

FIG. 1.—N_2H^+ $J = 1 \rightarrow 0$ spectra plotted as a function of distance from the Orion-KL/IRc2 position ($\alpha = 5^h32^m46^s.7$; $\delta = 5°24'23''.0$). For each spectrum, the velocity scale is shown, and measured velocities are given in the upper left. The temperature scale, in T_A^*, is given at the lower left of the figure. Toward the N and NE of IRc2, the 9.5 km s^{-1} velocity component dominates the spectra; toward the NW and W, the 7.2 km s^{-1} velocity is more apparent. The 9.5 and 7.2 km s^{-1} components are both present within $\sim 15''$ of IRc2.

© American Astronomical Society • Provided by the NASA Astrophysics Data System

1993ApJ...406L..29W

TABLE 1

OBSERVATIONS OF N_2H^+ $J = 1 \rightarrow 0$ TOWARD ORION-KL

Position[a] ($\Delta\alpha$, $\Delta\delta$)	T_A^* (K)			V_{LSR} (km s^{-1})	$\Delta v_{1/2}$ (km s^{-1})
	$F_1 = 0$–1	$F_1 = 2$–1	$F_1 = 1$–1		
(60, 60)	1.30	3.01	3.01	9.74 ± 0.20	1.02 ± 0.15
(60, 30)	...	<0.60	...	...	...
(60, 0)	...	<0.60	...	...	...
(60, −30)	...	<0.60	...	...	...
(60, −60)	...	<0.48	...	...	...
(30, 60)	2.12	3.46	2.70	9.79 ± 0.20	0.95 ± 0.15
(30, 30)	0.42	1.25	1.05	9.35 ± 0.20	0.91 ± 0.15
(30, 0)	...	<0.40	...	...	...
(30, −30)	...	<0.28	...	...	...
(30, −60)	...	<0.29	...	...	...
(0, 60)	<0.33	1.64	0.85	9.31 ± 0.20	1.02 ± 0.15
(0, 30)	0.60	1.68	1.14	9.47 ± 0.20	1.28 ± 0.30
(0, 0)	<0.15	0.45	0.29	9.28 ± 0.25	1.30 ± 0.30
(0, 0)	<0.15	0.46	0.24	7.34 ± 0.25	1.30 ± 0.30
(0, −30)	0.73	1.73	1.15	8.10 ± 0.25	0.95 ± 0.15
(0, −60)	0.74	2.35	1.41	6.51 ± 0.25	1.62 ± 0.30
(−30, 60)	1.29	2.58	2.22	7.39 ± 0.20	1.02 ± 0.15
(−30, 30)	1.43	3.48	2.80	7.39 ± 0.20	1.02 ± 0.15
(−30, 0)	0.45	1.65	1.21	7.07 ± 0.25	0.95 ± 0.15
(−30, −30)	0.45	1.18	0.60	6.28 ± 0.30	1.02 ± 0.15
(−30, −30)	<0.31	1.48	0.83	7.72 ± 0.30	1.02 ± 0.15
(−30, −60)	<0.40	1.18	0.80	7.07 ± 0.25	1.27 ± 0.20
(−60, 60)	1.74	4.80	3.39	7.66 ± 0.20	0.95 ± 0.15
(−60, 30)	1.54	3.32	3.14	7.40 ± 0.20	1.02 ± 0.15
(−60, 0)	0.41	1.44	0.95	7.05 ± 0.20	1.25 ± 0.20
(−60, −30)	0.26	0.97	0.73	6.75 ± 0.25	0.95 ± 0.15
(−60, −60)	...	<0.31	...	...	...
(−15, 15)	0.99	2.26	1.81	7.22 ± 0.20	1.02 ± 0.15
(−15, 15)	0.31	0.64	0.43	9.43 ± 0.20	1.02 ± 0.15
(−15, 0)	0.45	1.08	0.77	7.05 ± 0.35	0.95 ± 0.15
(−15, 0)	<0.22	0.56	0.47	9.05 ± 0.35	1.02 ± 0.15
(−15, −15)	0.37	0.83	0.57	6.49 ± 0.35	1.29 ± 0.30
(−15, −15)	0.40	1.18	0.85	8.38 ± 0.35	1.50 ± 0.30
(0, 15)	0.38	1.21	0.94	9.55 ± 0.20	1.02 ± 0.15
(0, 15)	<0.20	0.66	0.61	7.33 ± 0.20	0.95 ± 0.15
(0, −15)	<0.23	0.97	0.78	8.29 ± 0.30	1.20 ± 0.20
(15, 15)	<0.27	1.31	0.91	9.85 ± 0.20	1.20 ± 0.20
(15, 0)	...	<0.38	...	...	...
(15, −15)	<0.30	0.51	0.39	7.78 ± 0.35	1.20 ± 0.20

[a] Offsets are in arcseconds with respect to the coordinates $\alpha = 5^h32^m46^s.7$; $\delta = 5°24'23''.0$ (1950.0).

s^{-1} and $\Delta v_{1/2} \sim 2.5$ km s^{-1} (e.g., Ziurys, Wilson, & Mauersberger 1990).

Two models have been proposed to explain the velocity shift from ~7 km s^{-1} in the SW to ~10 km s^{-1} in the NE of the extended ridge gas. Differential rotation of the ridge along a SW–NE axis about KL has been suggested (Liszt et al. 1974; Hasegawa et al. 1984; Vogel et al. 1985). Alternatively, it has been proposed that the ridge is comprised of two or more distinct clouds which may overlap along the line of sight (Ho & Barrett 1978; Bastien et al. 1981, 1983; Womack et al. 1991).

To determine if the data are consistent with the rotation model, the N_2H^+ velocities along the central 30″ wide path of the ridge from 80″ SW to 80″ NE have been plotted as a function of distance from IRc2 (Fig. 2). The position angle of the cut is ~35°, consistent with estimates of a disk in rotation about IRc2 perpendicular to the axis of the bipolar outflows (e.g., Hasegawa et al. 1984; Murata et al. 1991). If rotation were present, the spectra should show a systematic change in velocity from ~8 km s^{-1} in the SW to ~10 km s^{-1} in the NE, tapering off on either end to the bulk cloud velocity of ~9 km s^{-1}, as proposed by Vogel et al. (1985). As demonstrated clearly in Figure 2, while there is an overall change from ~7.2 km s^{-1} SW of IRc2 to ~9.5 km s^{-1} in the NE, there is no systematic velocity gradient along the SW–NE axis. In fact, it is difficult to see any preferred axis of rotation in the extended ridge. For example, in the NE, cloud velocities are ~9.7 km s^{-1} at (60, 60), ~9.4 at (30, 30), ~9.9 km s^{-1} at (15, 15), and ~9.3 km s^{-1} at (0, 0). Similar variations in velocity are present in the 7.2 km s^{-1} cloud.

Furthermore, there is an abrupt jump in velocity from ~7.4 km s^{-1} at (−30, 60) and (−30, 30) to ~9.4 km s^{-1} at (0, 60) and (0, 30). This is difficult to explain with the rotation model, because the change in velocity occurs 30″ to 60″ NW of IRc2 (the proposed center of the rotation). If the NW velocity discontinuity represented the receding and approaching edges of a rotating cloud, then a similar jump should be symmetrically positioned 30″–60″ SE of the infrared object. Instead, no extended ridge emission is detected 30″–60″ to the SE of IRc2, as Figure 1 and Table 1 show.

To illustrate the inconsistency between the rotation model and the observations further, we computed radial velocities (V_R) for a differentially rotating spherical cloud about a central

© American Astronomical Society • Provided by the NASA Astrophysics Data System

1993ApJ...406L..29W

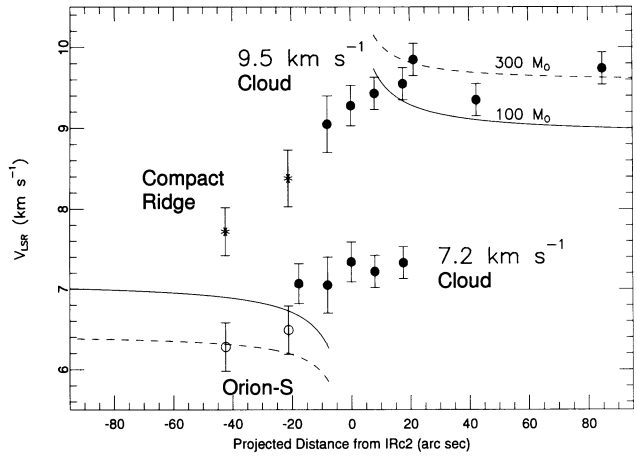

FIG. 2.—Observed radial velocities of N_2H^+ emission along the SW–NE direction (hypothetical rotation axis) of the extended ridge are plotted as a function of distance from IRc2. Velocities attributed to the 9.5 and 7.2 km s^{-1} clouds are denoted with filled circles, those of the compact ridge with asterisks, and data from Orion-S with open circles. Computed radial velocities for differentially rotating cloud models are plotted in solid and dashed lines. The observed velocities are completely inconsistent with the rotating cloud hypothesis, but are explained by the presence of four separate cloud clumps.

stellar mass, $M_* \sim 25\ M_\odot$, according to the equation

$$V_R = V_0 + \sin i\{G[M_* + (M_c/R_c)R]/R\}^{1/2} ,$$

where V_0 is the bulk velocity of the cloud (taken to be 8.4 km s^{-1}), G is the gravitational constant, R is the distance from the center of the cloud, i is the inclination of the cloud with respect to the line of sight, M_c is the total cloud mass, and R_c is the total cloud radius. This model assumes that the cloud's mass increases linearly with radius from the central stellar mass. Velocities were calculated for a rotating cloud of $M_c = 100\ M_\odot$ (*solid line*) and $300\ M_\odot$ (*dashed line*), assuming $i = 35°$ and $R_c = 45''$, parameters typically assigned to the proposed rotating ridge (e.g., Hasegawa et al. 1984; Vogel et al. 1985; Murata et al. 1991). The results are plotted along with the observed velocities in Figure 2. If the quiescent gas were in differential rotation about IRc2, then the model lines should be in agreement with the observed radial velocities. Instead, the data appear to have a small dispersion about a velocity of either 7.2 km s^{-1} or 9.5 km s^{-1}, with some extra points arising from the compact ridge and Orion-S.

Therefore, the N_2H^+ velocities are completely inconsistent with large-scale (1′–2′) differential rotation of the extended ridge gas about IRc2. Instead, the data strongly support the two-cloud model of KL first proposed by Ho & Barrett (1978). In addition, a similar velocity structure is seen in spectra of CH_3CCH consistent with multiple cloud components (Wang, Wouterloot, & Wilson 1993).

4.2. *Implications for Star Formation*

It is noteworthy that at the projected juncture of the two major clouds of quiescent gas there are molecular outflows, masers, several compact infrared sources, and at least one young stellar object, IRc2. The line-of-sight velocity difference between the two clouds is ~ 2.2 km s^{-1}, which is similar to the characteristic velocity dispersion between cloud clumps in other star-forming regions (Pérault, Falgarone, & Puget 1985; Stutzki & Güsten 1990; Evans, Kutner, & Mundy 1987). Thus it is possible that star formation at Orion-KL may have been triggered by a cloud-cloud interaction.

Alternatively, star formation may have begun by another method, and the resulting outflowing material may be plowing into the quiescent gas, pushing apart the two regions of the ridge and producing the observed velocity difference. The kinetic energy needed to push apart two 50 $M_\odot$ clumps at 1.1 km s^{-1} is $\sim 10^{45}$ ergs. Interestingly, this is comparable to the energy of (2–30) $\times\ 10^{45}$ ergs thought to be expended by the high-velocity molecular outflows within 100″ of IRc2 (Martín-Pintado et al. 1990; Snell et al. 1984).

Recent observations indicate that molecular clouds are not whole, homogeneous quantities, but rather consist of smaller (< 1 pc) clumpy components of gas and dust (e.g., Howe et al. 1991; Parmar, Lacy, & Achtermann 1991). Small-scale clumping of material is expected to have a significant impact on the chemistry of young star-forming environments (Burton, Hollenbach, & Tielens 1990; Howe et al. 1991; Stutzki et al. 1988). Therefore, in order to describe the physical and chemical conditions influencing stellar birth, it is crucial to study the surrounding cloud structure in greater detail.

4.3. *Implications for Chemistry of Molecular Ions*

Most chemical models of dense clouds predict that molecular ions are produced through ion-molecule reactions in cold, quiescent gas and destroyed largely by dissociative electron recombination, especially in regions of hot, perturbed gas (Brown & Rice 1986; Herbst & Leung 1986; Langer & Graedel 1989; Millar 1990). Studies of N_2H^+ in molecular clouds have found that its emission is characterized by narrow line widths ($\Delta v_{1/2} \sim 1$–5 km s^{-1}) and low excitation temperatures ($T_{ex} <$ 20 K), in agreement with models of molecular ion chemistry (e.g., Womack et al. 1992). Interestingly, Figure 1 shows that N_2H^+ $J = 1 \rightarrow 0$ emission is significantly diminished within 30″ of IRc2, where the 9.5 and 7.2 km s^{-1} clouds overlap. This region contains hot, perturbed gas, young stellar object(s) and molecular outflows. While most chemical models predict that molecular ions should be destroyed in hot, perturbed gas, this of N_2H^+ emission may be an excitation effect. As gas temperature and density increase, the higher rotational levels of a molecule should become more populated. In fact, measurements of the N_2H^+ $J = 3 \rightarrow 2$ transition toward IRc2 obtained with the same beamwidth (Womack et al. 1991) indicate a line radiation temperature 5 times stronger than the $J = 1 \rightarrow 0$ measurement presented in this *Letter*. The observed relative strengths of the $J = 1 \rightarrow 0$ and $J = 3 \rightarrow 2$ transitions are consistent with the population distribution expected for N_2H^+ in the hot, dense gas surrounding IRc2. Therefore, the decrease of N_2H^+ $J = 1 \rightarrow 0$ emission may be indicative of a different relative population of rotational levels in hotter, denser gas, rather than a lower abundance of the ion. Further observations are needed to better understand the behavior of molecular ions in hot, dense gas.

5. CONCLUSIONS

A map of emission from the N_2H^+ $J = 1 \rightarrow 0$ transition, at 26″ resolution, was made of the Orion-KL region. The spectra exhibit several narrow velocity components and indicate the presence of at least four quiescent clouds near IRc2. The measured velocities do not change uniformly across OMC-1 and are completely inconsistent with large-scale ($\sim$1′–2′) differential rotation of the extended ridge gas about IRc2. The data are explained by cloud clumping and overlap and suggest that

© American Astronomical Society • Provided by the NASA Astrophysics Data System

1993ApJ...406L..29W

either star formation has been initiated by a cloud-cloud collision or that two clouds are being pushed apart by energetic phenomena.

A significant decrease of N_2H^+ $J = 1 \rightarrow 0$ emission is observed within 30″ of IRc2. This may be due to the chemistry in hot, dense gas, or it may be an excitation effect.

The authors would like to thank T. L. Wilson for helpful discussions. The North Atlantic Treaty Organization is acknowledged for partial support of this project. L. M. Z. also acknowledges NSF grants AST-90-58467 and AST-91-10701 and NASA grant NAGW 3065.

REFERENCES

Bastien, P., Batrla, B., Henkel, C., Pauls, T., Walmsley, C. M., & Wilson, T. L. 1985, A&A, 146, 86
Bastien, P., Bieging, J., Henkel, C., Martin, R. N., Pauls, T., Walmsley, C. M., Wilson, T. L., & Ziurys, L. M. 1981, A&A, 98, L4
Blake, G. A., Sutton, E. C., Masson, C. R., & Phillips, T. G. 1987, ApJ, 315, 621
Brown, R. D., & Rice, E. H. N. 1986, MNRAS, 223, 405
Burton, M., Hollenbach, D. J., & Tielens, A. G. G. M. 1990, ApJ, 365, 620
Cazzoli, G., Corbelli, G., Degli Esposti, C., & Favero, P. G. 1985, Chem. Phys. Letters, 118, No. 2, 164
Downes, D., Genzel, R., Becklin, E. E., & Wynn-Williams, C G. 1981, ApJ, 244, 869
Evans, N. J., Kutner, M. L., & Mundy, L. G. 1987, ApJ, 323, 145
Friberg, P. 1984, A&A, 132, 265
Hasegawa, T., et al. 1984, ApJ, 283, 117
Herbst, E., & Leung, C. M. 1989, ApJS, 69, 271
Ho, P. T. P., & Barrett, A. H. 1978, ApJ, 24, L23
Howe, J. E., Jaffe, D. T., Genzel, R., & Stacey, G. J. 1991, ApJ, 373, 158
Johnston, K. J., Gaume, R., Stolovy, S., Wilson, T. L., Walmsley, C. M., & Menten, K. M. 1992, ApJ, 385, 232
Langer, W. D., & Graedel, T. E. 1989, ApJS, 69, 241
Liszt, H. S., Wilson, R. W., Penzias, A. A., Jefferts, K. B., Wannier, P. G., & Solomon, P. M. 1974, ApJ, 190, 557
Mangum, J. G., Wootten, A., Loren, R. B., & Wadiak, E. J. 1990, ApJ, 348, 542
Martín-Pintado, J., Rodríguez-Franco, A., & Bachiller, R. 1990, ApJ, 357, L49
Millar, T. J. 1990, in Molecular Astrophysics, ed. T. W. Hartquist (Cambridge: Cambridge Univ. Press), 115
Murata, Y., Kawabe, R., Ishiguro, M., Hasegawa, T., & Hayashi, M. in Fragmentation of Molecular Clouds and Star Formation, ed. E. Falgarone et al. (Dordrecht: Kluwer), 357
Parmar, P. S., Lacy, J. H., & Achtermann, J. M. 1991, ApJ, 372, L25
Pérault, M., Falgarone, E., & Puget, J. L. 1985, A&A, 152, 371
Snell, R., Scoville, N. Z., Sanders, D. B., & Erikson, N. R. 1984, ApJ, 284, 176
Stutzki, J., & Güsten, R. 1990, ApJ, 356, 513
Stutzki, J., Stacey, G. J., Genzel, R., Harris, A. I., Jaffe, D. T., & Lugten, J. B. 1988, ApJ, 332, 379
Vogel, S. N., Bieging, J. H., Plambeck, R. L., Welch, W. J., & Wright, M. C. H. 1985, ApJ, 296, 600
Wang, T. Y., Wouterloot, J. G. A., & Wilson, T. L. 1993, in preparation
Womack, M., Ziurys, L. M., Wyckoff, S. 1991, 370, L99
———. 1992, 387, 417
Ziurys, L. M., Wilson, T. L., & Mauersberger, R. 1990, ApJ, 356, L25

© American Astronomical Society • Provided by the NASA Astrophysics Data System